International Journal of Engineering Applied Sciences and Technology, 2021
Vol. 6, Issue 8, ISSN No. 2455-2143, Pages 200-209
Published Online December 2021 in IJEAST (http://www.ijeast.com)

MODELING OF REDUCTION OF ITAKPE OXIDE PELLETS IN FURNACE REACTOR

Olayebi. O
Department of Chemical Engineering ,
Federal University of Petroleum Resources,
Effurun, Delta State, Nigeria

Ogbeide S. E
Department of Chemical Engineering,
University of Benin, Benin City, Edo state
Nigeria

ABSTRACT - The multiple gas solid reactions, the physico-chemical, transport and thermal phenomena taking place in the Direct reduction furnace of the Delta Steel plant was modelled using the shrinking core model on Itakpe ore with a view to improving on the efficiency of the reduction process. The mathematical description of the detailed physical, chemical, transport and thermal phenomena occurring in the furnace was carried out and the models described the fluid/solid flows through the moving bed reactor system and was conjugated with heat transfer, specie transport which included the solid oxide pellet feed and the reducing gases. The effect of the diffusion resistances, the intra-particle diffusion and kinetic phenomena coupled with other operating parameters on the overall particle conversion were examined and the Shrinking Core Model was able to correctly describe the heterogeneous process. The models were validated with data obtained in the reduction of the local Itakpe iron ore pellets. The simulated particles in this process was the 1.2cm diameter Itakpe pellet. The results of the reduction of the Itakpe iron ore were in close conformance with the behaviour of most worldwide iron oxides used in the direct reduction process.

K*ey words*: Direct Reduction, Itakpe Iron ore, Modeling, One Interface.

I. INTRODUCTION

The importance of iron and steel as a basis for technological development is common knowledge and all industrialized nations have multiple iron and steel plants, some of which are integrated.
As a result, under the auspices of the Nigerian Steel Development Authority (NSDA), Nigerian and Soviet geologists and technologists were able to determine the resources and suitable local raw materials required to set up an integrated iron and steel plant at Ajaokuta in Kogi State.

Although the main contract for the establishment of the conventional Blast Furnace – Basic Oxygen Furnace route to steel production was signed in 1979, global recession, poor funding and the installation of massive infrastructural facilities had stood on the way of the completion and full commissioning of Africa's largest steel making Plant.

The Delta Steel Direct Reduction – Electric Arc Furnace route to Steel production was established to meet the steel needs and also to put Nigeria on the map of the world as a major steel producer, against the backdrop of the delay in the completion and commission the Ajaokuta Steel Project.

The decision by the Federal Government to adopt the direct reduction process was hinged on the abundant natural gas in the Niger Delta region of the country thereby making the import of coal which was an essential ingredient for the conventional blast furnace process unnecessary. Also, investment cost was lower and flexibility of operation with respect to variation of operating parameters with regard to different iron ore qualities was plausible [1].

Direct reduced iron and specifically that produced through the Midrex process is a highly metallized type of direct reduced iron with known and controlled chemical characteristics and helps in meeting the demand for the production of quality steel from the Electric Arc Furnaces.

This is because, the effect of DRI on the physical properties of steel can increase productivity and yield in the rolling mills and downstream of the manufacturing facilities.

At Delta Steel Company, the quantity of DRI charged to the melting furnace ranges from 70 – 80 % which necessitates the need to produce optimum quality DRI. The Lamco Liberian/Guinean ore based on which the Direct Reduction plant at Delta Steel was designed, was successfully reduced with

International Journal of Engineering Applied Sciences and Technology, 2021
Vol. 6, Issue 8, ISSN No. 2455-2143, Pages 200-209
Published Online December 2021 in IJEAST (http://www.ijeast.com)

Performance Guarantee Test values meeting the designed values.

II. DIRECT REDUCTION AT DELTA STEEL

Itakpe Iron Ore

Upon commissioning of the Delta Steel Company and subsequent commercial production of steel, the Liberian/Guinean ore mines from where the Lamco iron ore used as feedstock for the Direct Reduction Plant at Delta Steel, and on the basis of which the plant was designed, was depleted within 3 years of commissioning.

This led to the necessity to seek other sources of raw materials. The next alternatives were the Brazilian Compania Vale do Rio Doce (CVRD) and Feijaio Ores which apart from the peculiarity in their operational characteristics were not readily available due to scarce foreign exchange. These ores were used sparingly between 1989 and 1993.

It therefore became imperative to seek other sources of iron ore. This led to the need to investigate the possibility of utilizing at Delta Steel Company, the locally available iron ore in Itakpe in Kogi state of Nigeria, which was originally conceived for use at the Blast Furnace plant in Ajaokuta. This plant was built to accommodate sinter grade of 63 to 64% total iron content. The silica was in excess of 4% and the ore was not suitable for the Direct Reduction process at DSC [2].

The beneficiation of Itakpe iron ore, making it suitable for production of Direct Reduced Iron from the MIDREX based Direct Reduction Plant at Delta Steel Company, marked a major turning point in the historical quest for the production of iron and steel from locally available iron oxide raw material in Nigeria.

Itakpe is a rural area situated in Okene local Government area of Kogi state in central Nigeria, lying within the latitudes $7^{O}36'N$ to $7^{O}39'N$ and longitudes $6^{O}17'E$ to $6^{O}22'E$ shown in Figure 1.

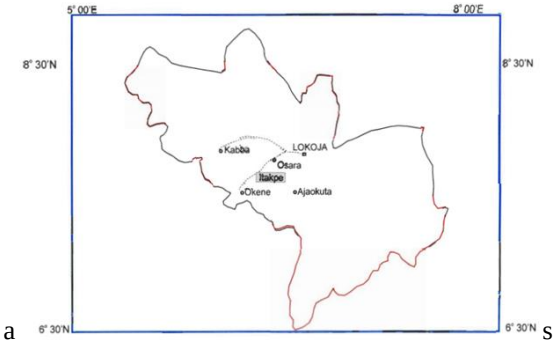

a s

Figure 1: Map showing location of Itakpe in Kogi State. Source: [3]

The Itakpe iron ore deposit is located about 16 km northeast of Okene town in Kogi
state and is reported to form a series of iron-bearing quartzites ridge in that area. This
ridge is approximately 1 km wide and 5 km in length and reaching a maximum
elevation of about 500 m above the surrounding low land with the deposit consisting of eastern and western mines [4]. The Itakpe iron-ore deposit is localized within the gneiss-migmatite quartzite unit [5].
Figure 2 shows a sample of Itakpe iron ore.

Figure 2: Itakpe Iron Ore sample

Direct Reduction Process at Delta Steel

The direct reduction ironmaking plant at the Delta Steel Company are two MIDREX Process based 600 series 5.5m diameter modules each with an annual production capacity of 510,000 Tonnes of direct reduced iron (DRI).
The DRI is used mainly as the raw material for the in-house electric arc furnaces (EAFs), as a clean iron

International Journal of Engineering Applied Sciences and Technology, 2021
Vol. 6, Issue 8, ISSN No. 2455-2143, Pages 200-209
Published Online December 2021 in IJEAST (http://www.ijeast.com)

source. The Midrex process flow sheet is shown in Figure 3.

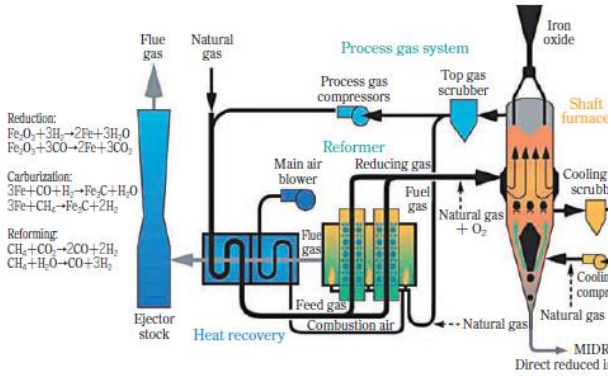

Figure 3: Midrex Direct Reduction flowsheet. Source: [6].

The Reduction Shaft Furnace

The furnace structure is shown in Figure 4 and is divided into two major parts namely:

i The Reduction zone
ii The Cooling zone

In the Furnace, the iron oxide feed material comes in contact with a countercurrent flow of hot reducing gases and is reduced to metallic iron.

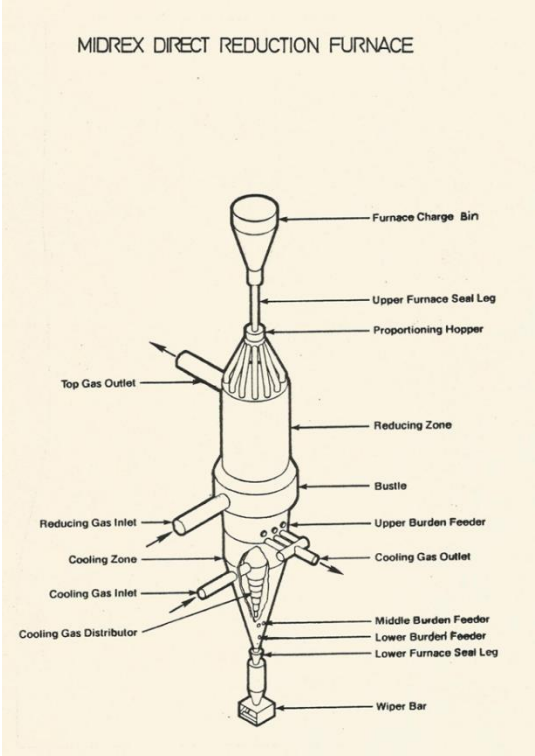

Figure 4: Reduction Shaft Furnace. (Source: [7]

III. MODELING WITH MATLAB

The MATLAB 5.0 software was used in solving the governing equations.

3.1 Model for Moving Bed Reactors

The shrinking core model was applied on a one interface basis.

Figure 5 shows the schematic representation of the moving – bed reactor which consists of porous solid pellets with an exploded schematic of a pellet based on the shrinking core model, illustrating the concentric layers as the reaction progresses.

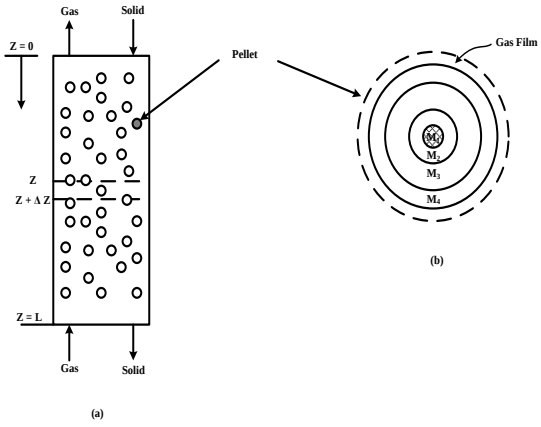

Figure 5: Moving Bed Reactor with Porous Pellets

The aspects under consideration include heat and mass transfer. In approaching the analysis, kinetic models were employed.

International Journal of Engineering Applied Sciences and Technology, 2021
Vol. 6, Issue 8, ISSN No. 2455-2143, Pages 200-209
Published Online December 2021 in IJEAST (http://www.ijeast.com)

The model was applied to the reduction of iron oxide (hematite) pellets in the moving Bed of the Direct Reduction Plant Shaft Furnace which involves multiple non – catalytic gas – solid reactions for the one interface model.

3.2 One interface model

The one interface model also known as the progressive core model was applied to the global kinetics. Under this consideration, the reduction of the initial iron oxide progressed directly to iron. The reactions of interest are as follows:

$$Fe_2O_3 + 3H_2 \rightarrow 2Fe + 3H_2O \qquad (1)$$

$$Fe_2O_3 + 3CO \rightarrow 2Fe + 3CO_2 \qquad (2)$$

These are re-written as:

$$\frac{1}{3}Fe_2O_3(s) + H_2(g) \rightarrow \frac{2}{3}Fe(s) + H_2O(g)$$

$$\frac{1}{3}Fe_2O_3(s) + CO(g) \rightarrow \frac{2}{3}Fe(s) + CO_2(g)$$

3.3 Governing Equations

3.3.1 Equations used for conversion

The reactant gas species in the bulk phase are transported through the gas-film surrounding the pellet, and through the layer of porous solid-product to the iron-oxide interface where it reacts. Each of the product gas specie follows a similar inverse path from the reacting surface to the bulk fluid phase.

The extent of reaction was defined in terms of the concentration changes occurring in the gas phase as follows [8] :

$$C_j = C_j^o + \sum_i \alpha_{ij} X_i \qquad (3)$$

For each species *j* and where α_{ij} is the stoichiometric coefficient.
With respect to the gaseous phase,

$$X_1 = C_{H_2}^o - C_{H_2} \qquad (4)$$

$$X_2 = C_{CO}^o - C_{CO} \qquad (5)$$

where the first terms stand for the initial concentration of the components.

The concentration equation was broken down as follows:

$$C_{H_2} = C_{H_2}^0 + \left[\alpha_{H_2}^1 X_1\right] \qquad (6)$$

$$C_{CO} = C_{CO}^0 + \left[\alpha_{CO}^2 X_2\right] \qquad (7)$$

Now, $\alpha_{H_2}^1$ and α_{CO}^2 = -1

$$C_{H_2} = C_{H_2}^0 - X_1 \quad \Rightarrow \quad X_1 = C_{H_2}^0 - C_{H_2} \qquad (8)$$

$$C_{CO} = C_{CO}^0 - X_2 \quad \Rightarrow \quad X_2 = C_{CO}^0 - C_{CO} \qquad (9)$$

For the solid phase,

$$X_{rs} = X_1 + X_2 = 3\left[C_{Fe_2O_3}^o - C_{Fe_2O_3}\right] \equiv X_3 \qquad (10)$$

The shrinking core model was used for the solid pellet. The corresponding reaction rate expression per pellet is given by [8]):

$$\hat{R} = \frac{-4\pi r_c^2 C_n}{\left(1/k_n + r_c/D_n - r_c^2/r_0 D_n\right)} \qquad (11)$$

where, n stands for the reactants H_2 and CO.

The reaction rate for the entire process is expressed as,

$$R = n_p \hat{R}$$

3.3.2 Mass balance for gas phase

The mass balance for the gas phase was obtained through the following expressions:

$$\frac{dX_1}{dz} = -\frac{n_p}{u}\hat{R}_1\left(X_1, X_3\right) \qquad (12)$$

$$\frac{dX_2}{dz} = -\frac{n_p}{u}\hat{R}_2\left(X_2, X_3\right) \qquad (13)$$

These are expanded as follows:

$$u\frac{dX_{H_2}}{dz} + n_P\hat{R}_{H_2}\left(X_{H_2}, X_s\right) = 0 \qquad (14)$$

Also,

$$u\frac{dX_{CO}}{dz} + n_P\hat{R}_{CO}\left(X_{CO}, X_s\right) = 0 \qquad (15)$$

International Journal of Engineering Applied Sciences and Technology, 2021
Vol. 6, Issue 8, ISSN No. 2455-2143, Pages 200-209
Published Online December 2021 in IJEAST (http://www.ijeast.com)

3.3.3 Energy balance for gas phase

The energy balance for gas phase is given as follows:

$$\frac{dT_g}{dz} - \frac{n_P A_P h\left(T_{sol} - T_g\right)}{G m_g C_{P_g}\left(X_1, X_2, T_g\right)} = 0 \qquad (16)$$

This can be expressed as,

$$\frac{dT_g}{dz} - \frac{n_P A_P h\left(T_{sol} - T_g\right)}{G m_g C_{P_g}\left(X_{H_2}, X_{CO}, T_g\right)} = 0 \qquad (17)$$

3.3.4 Heat transfer coefficient

The correlation used to obtain the heat transfer coefficient is given as [9]:

$$Nu = 2 + 0.6 \mathrm{Re}^{1/2} \mathrm{Pr}^{1/3} \qquad (18)$$

3.3.5 Thermal conductivity of gases

Correlations are available [10] for the evaluation of polar, non-polar, linear and non-linear gases. For non-polar and linear gases like hydrogen, carbon monoxide and carbon dioxide, the following correlation was applied:

$$\frac{\lambda_g MW}{\mu C_v} = 1.30 + \left(\frac{R}{C_v}\right)\left[1.7614 - \frac{0.3523}{T_r}\right] \qquad (19)$$

For non-linear gases like steam which is one of the product gases, the applicable correlation is:

$$\frac{\lambda_g M}{\mu C_v} = 1.30 + \left(\frac{R}{C_v}\right) \qquad (20)$$

where R is the universal gas constant and T_r is reduced temperature

The Bulk thermal conductivity denoted by λ_g was obtained from the following relationship:

$$\lambda_g = \frac{\sum_i Y_i M_i^{1/3} \lambda_{g,i}}{\sum_i Y_i M_i^{1/3}} \qquad (21)$$

3.3.6 Mass balance for solid phase

The governing equation for the mass balance for the oxide feed is as follows:

$$\frac{dX_3}{dz} = -\frac{n_p}{u_s}\left[\hat{R}_1 + \hat{R}_2\right] \qquad (22)$$

This was applied, knowing that velocity of the solid is u_S as follows:

$$u_S \frac{dX_S}{dz} + n_P\left[\hat{R}_{H_2}\left(X_{H_2}, X_S\right) + \hat{R}_{CO}\left(X_{CO}, X_S\right)\right] = 0 \qquad (23)$$

3.3.7 Energy balance for oxide feed

The governing equation for the energy balance for the oxide feed is as follows:

$$\frac{dT_S}{dz} - \frac{n_P}{G m_S(X_S) C_{P_S}(X_S, T_S)} X\left[A_p h\left(T_S - T_g\right) - \sum_i \Delta H_i(T_S)\hat{R}_i\left(X_i, X_S, T_S\right)\right] = 0 \qquad (24)$$

This equation was applied taking into account the gaseous reactants, hydrogen and carbon monoxide respectively to give,

$$\frac{dT_S}{dz} - \frac{n_P}{G m_S(X_S) C_{P_S}(X_S, T_S)} X\left[A_p h\left(T_S - T_g\right) - \sum_{H_2} \Delta H_{H_2}(T_S)\hat{R}_{H_2}\left(X_{H_2}, X_S, T_S\right)\right] = 0 \qquad (25)$$

and

$$\frac{dT_S}{dz} - \frac{n_P}{G m_S(X_S) C_{P_S}(X_S, T_S)} X\left[A_p h\left(T_S - T_g\right) - \sum_{CO} \Delta H_{CO}(T_S)\hat{R}_{CO}\left(X_{CO}, X_S, T_S\right)\right] = 0 \qquad (26)$$

The specific heat capacity of the solid, C_{P_S} is the weighted average of the specific heat capacity of the initial solid feed and that of the solid product according to the following expression,

$$C_{P_S} = \frac{\left[C_{P_{s,feed}} \rho_{s,feed} r_c^3 + C_{P_{s,prod}} \rho_{s,prod}\left(r_0^3 - r_c^3\right)\right]}{\left[\rho_{s,feed} r_c^3 + \rho_{s,prod}\left(r_0^3 - r_c^3\right)\right]} \qquad (27)$$

Based on the theoretical considerations for the unreacted shrinking core model and that the concentration of reactive solid must be measured per unit of reactor volume, it was possible to relate the

International Journal of Engineering Applied Sciences and Technology, 2021
Vol. 6, Issue 8, ISSN No. 2455-2143, Pages 200-209
Published Online December 2021 in IJEAST (http://www.ijeast.com)

radius of the unreacted core (r_c) as it varies with the solid conversion (X_3) through equation (28).

$$r_c = \left(r_0^3 - \frac{X_3 M_w}{n_P 4\pi\rho} \right)^{1/3} \qquad (28)$$

The number of pellets entering the reactor per unit time (n_p) was expressed as follows [11]:

$$n_p = \frac{3P_S}{4\pi R_P^3 \rho_S \left(1-\varepsilon_p\right) M_{ws}} \qquad (29)$$

M_{ws} is the molecular weight of solid pellet feed (kg/mol)

The rate of conversion of the solid feed is affected by the rate of production which is equivalent to the molar flow of the solid and can be expressed as follows:

$$G_{m_S}(r_c) = G_{m_S}^L \frac{\left[1/2\, r_c^3 \rho_{s,feed} / M_{w_{s,feed}} + \left(r_0^3 - r_c^3\right)\rho_{s,prod} / M_{w_{s,prod}} \right]}{\left[r_c^3 \rho_{s,feed} / M_{w_{s,feed}} + \left(r_0^3 - r_c^3\right)\rho_{s,prod} / M_{w_{s,prod}} \right]} \qquad (30)$$

3.3.8 Heat of Reaction

Based on reactions taking place between reactants and the resulting products, generally the heat of reaction was calculated using the following equation [12]:

$$\Delta H_{Prods} - \Delta H_{Reacts} = \left(n_{P1}\Delta\hat{H}_{P1}^{o} + n_{P2}\Delta\hat{H}_{P2}^{o}\right) - \left(n_{R1}\Delta\hat{H}_{R1}^{o} + n_{R2}\Delta\hat{H}_{R2}^{o}\right) + \int_{T_{Ref}}^{T_{out}} \left(n_{P1}C_{P1} + n_{P2}C_{P2}\right)dT - \int_{T_{Ref}}^{T_{in}} \left(n_{R1}C_{R1} + n_{R2}C_{R2}\right)dT \qquad (31)$$

where, P stands for products and R for reactants.

3.3.9 Boundary conditions

The analysis was carried out as a boundary value problem in which the conversions of the gases are predicted at the reducing gas outlet, which is the solid feed inlet, so as to satisfy the gas conversions at the outlet and the temperature of the inlet gases. The boundary conditions are,

$$\left.\begin{array}{l} X_{H_2}(Z=L)=0 \;\;,\;\; X_{CO}(Z=L)=0 \\ X_S(Z=0)=0 \;\;,\;\; T_g(Z=L)=T_g^{in} \\ T_S(Z=0)=T_{amb} \end{array}\right\} \qquad (32)$$

where T_{amb} is the ambient temperature.

3.4 Data used for Modeling and Simulation

The physico-chemical properties of the Itakpe pellets are presented in Table 1.

Table 1**:** Properties of Pellets Derived from Itakpe Iron Ore

Parameter	Prime Ore	Dsc Specification
GREEN PELLETS		
MOISTURE (%)	8.10	7 – 8.0
DROP NO (D/P)	5.7	4.8 min
CCS (N/P)	11.22	9.0 min
FIRED PELLETS PHYSICAL PROPERTIES		
CCS (N/P)	4561	3450
+ 16mm (%)	21.41	5.0 max
6.3 – 19m (%)	95.05	92.0 min
Tumble Index (%)	94.51	93.0 min
Abrasion Index (%)	3.93	5.0 max
Firing Temp (^{0}C)	1300	1300
CHEMICAL PROPERTIES		
Fe^{tot} (%)	65.10	66.00 min
Fe_2O_3 (%)	93.21	94.00 min
$SiO_2 + Al_2O_3$ (%)	4.57	3.50 max
CaO (%)	2.13	1.50 – 01.70
MgO	Trace	2.00 max
S	0.001	0.001 max
P.	N.D	0.03 max
	0.51	0.60 min

*CCS = Cold Compression Strength

International Journal of Engineering Applied Sciences and Technology, 2021
Vol. 6, Issue 8, ISSN No. 2455-2143, Pages 200-209
Published Online December 2021 in IJEAST (http://www.ijeast.com)

Table 2**:** Simulation parameters

Variable	Units
Furnace Dimension	
Reduction zone length	10 *m*
Reduction zone diameter	5.5 *m*
Iron oxide properties	
Total iron	68 %
Hematite (Fe_2O_3)	95.6 %
Density	3400 kg/m^3
Oxide pellet radius	6 cm
Direct reduced iron properties	
Bulk density	1700 kg/m^3
Pellet ratio	9900 pellets/m^3
Production rate	65 Tonnes/hr
Reducing gas parameters	
Flow rate	120,000 Nm^3/hr
Gas temperature	760 ^{O}C (1033 K)

Table 2**:** Simulation parameters (contd)

Gas properties	
H_2	52.85 %
CO	34.67 %
CH_4	4.10 %
H_2O	4.87 %
CO_2	2.84 %
N_2	0.67 %
Gas concentration	
C_{H_2O}	6.5510 x 10^{-6} kmol/cm^3
C_{CO}	4.285 x 10^{-6} kmol/cm^3
Kinetic constants	
k_{H_2}	0.225 exp(-147/82.06T) cm/s
k_{CO}	0.650exp(-28100/82.06T) cm/s
Diffusion coefficients	
D_{H_2}	1.467 x 10^{-6} T cm^2/s
D_{CO}	3.828 x 10^{-7} T cm^2/s
Heat transfer coefficient	1.67363.828 x 10^9 J/m^{2}sK

IV. RESULTS AND DISCUSSIONS

The shrinking core model assumes that the reaction is localized at an interface that moves from the external surface of the pellet to the center of the pellet while the reaction proceeds.

The equations for the gaseous reactants were solved with the assumption that the reaction occurs at the interface of the core and shell. It is also assumed that diffusion alone takes place in the layer between the reaction interface and the external surface of the pellet.

The composition of the Itakpe ore were used hence hematite which constitutes more than 94% of the oxide feed mixture was taken as the major feed material.

The differential equations were solved and the concentration and temperature profiles of gas and solid are presented in the application of the model to the reduction of the Itakpe iron oxide pellets with a diameter of 1.2cm. The graphs were plotted on the Excel Environment.

Change in Concentration of reactant gases

The changes in the concentration profiles for the gas phase indicate changes in composition which are caused by reactions taking place in the gas phase.

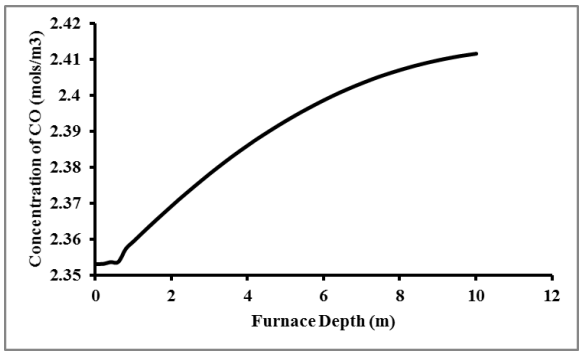

Figure 6: Concentration of carbon monoxide (CO) versus reduction zone length

It is observed that the concentration is higher at the exit of the reduction zone which is the inlet of the reducing gases.

International Journal of Engineering Applied Sciences and Technology, 2021
Vol. 6, Issue 8, ISSN No. 2455-2143, Pages 200-209
Published Online December 2021 in IJEAST (http://www.ijeast.com)

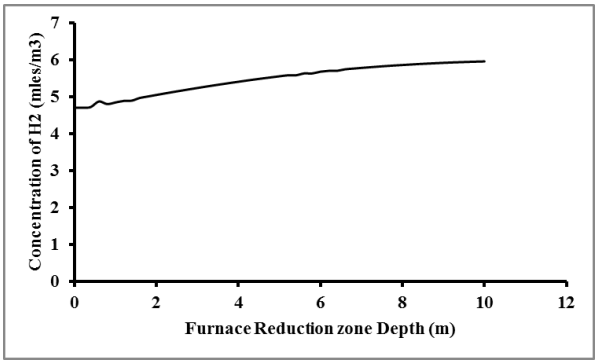

Figure 7: Concentration profile of hydrogen (H_2) versus reduction zone length

The profiles of the concentration profiles for the gas phase indicate changes in composition which are caused by reactions taking place in the gas phase.
It is also observed from Figure 7 that the concentration of hydrogen is higher at the exit of the reduction zone. The concentration profiles for both reactant gases are similar even though the concentration of the H_2 is greater than that of CO. The implication of this is that the differences in concentrations of the two components of the feed gas allows for both reducing gases to act simultaneously throughout the reactor, removing similar quantities of oxygen. Theoretically, on the basis of concentration only it can be deduced that CO reduction has advantage over H_2 since smaller concentrations of CO are usually required.

In general, more H_2 and CO will increase metallization and an increased bustle gas flow per tonne will ensure that the gas contacting the ore is further from equilibrium; and therefore, metallization or degree of conversion will increase.

Concentration profile of Hematite

The profile of the change in concentration of the hematite ore is shown in Figure (8)

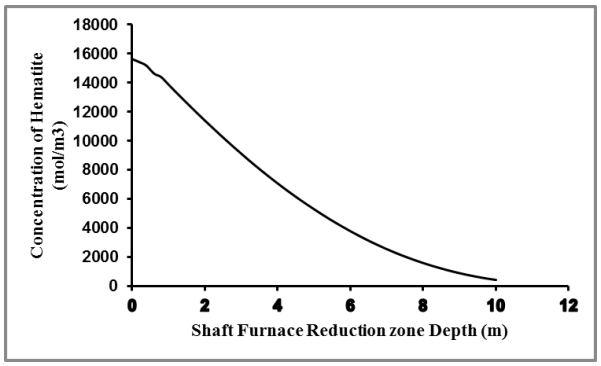

Figure 8: Change in concentration reactant solid feed (Hematite) versus shaft furnace reduction zone depth

The extent of reaction is found to be very high as should be expected at the bottom of the reduction zone. The gas and solid temperature profiles move in the opposite direction to each other. It is observed that the incoming solid phase rapidly reaches the much higher temperature of the gas phase at the top of the reduction zone.
It is to be observed that the reactant solid, hematite (Fe_2O_3) attain maximum reduction when it exits the reduction zone.

Temperature of Reducing gases and Oxide feed
It is noted that the higher the degree of reduction the higher is the metallization degree. Increasing the reduction gas inlet temperature leads to an enhancement of the reaction temperature and an acceleration of the reaction flow rate.
This is because the rate of iron ore reduction is intensified when there is an increase in temperature.
It is to be noted however that even though increasing the temperature can result in higher metallization degree, the physical properties of iron ore can be a limiting factor.

In this case temperature has to be maintained below the clustering temperature of the pellets. Clustering tends to result from the sintering of the pellets to each other which can lead to channeling in the reduction zone and eventual hot spots and also resulting in non-uniform product quality. The reduction temperature used in this work is below the clustering temperature of the Itakpe ore.

International Journal of Engineering Applied Sciences and Technology, 2021
Vol. 6, Issue 8, ISSN No. 2455-2143, Pages 200-209
Published Online December 2021 in IJEAST (http://www.ijeast.com)

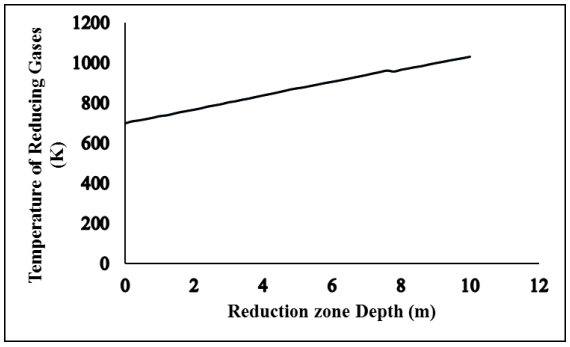

Figure 9: Temperature of reactant feed gas versus reduction zone depth

The profile of the temperature of reactant feed gas along the length of shaft furnace reduction zone length is shown in Figure 9. The temperature is highest at the exit into the reduction from where the gas is fed into the furnace. It is observed that there is tendency of uniformity of both profiles through the length of the reactor.

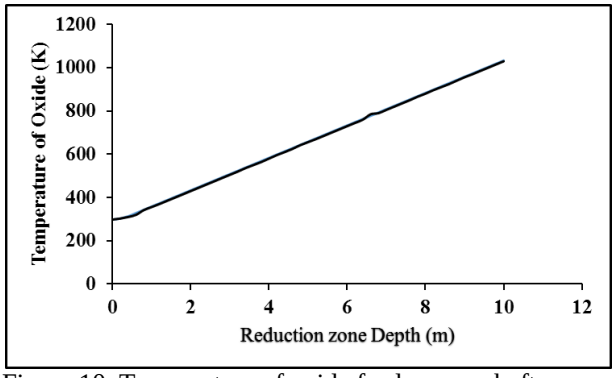

Figure 10: Temperature of oxide feed versus shaft furnace reduction zone depth

It is crucial to maintain proper burden temperature which depends on the temperature of the reducing gases as shown in Figure 10.
Higher reducing or bustle gas and burden temperatures favor reduction kinetically and thermodynamically.
The burden temperature will determine the equilibrium conditions for the reduction reaction at a given bustle gas analysis.

It is observed from Figures 9 and 10 that temperature profiles along the length of the reduction zone show an increase in gas and solid temperature from the top of the reduction zone which is the direction of the oxide flow. The same observation was made by [13].

The Figures show that the temperature profiles along reduction zone for both the gas and solid phases are in good agreement with what should be expected with respect to the inlet and outlet temperatures. It is observed that temperature profiles along reduction zone increase with increase in gas and solid temperatures in their countercurrent directions of flow.
Because some of the reduction reactions are endothermic, and some of the reduction reactions are exothermic, no general correlation of burden temperature with metallization can be given without also specifying the bustle gas composition. An increase in temperature favours the kinetics for both reduction reactions. It is observed that reduction or metallization degree increases with increase in gas inlet temperature. This is also stated by [13}. Also, [14] established that an increase in the reduction temperature resulted in an increase in the reduction rate. However, it is noted that an increase in rate may not mean an increase in metallization because of the complex effects of equilibrium on metallization.

With respect to considering the effect of temperature on metallization degree the inlet temperature of reduction gas is very crucial. The temperature range considered in the model accounts for the reduction temperatures that have been utilized for the Itakpe ore.
The inlet temperature in expected to be highest at the inlet of the reduction zone.
If the burden temperature becomes too high, the material may begin to agglomerate. However, a burden temperature that is too low can retard the rate of reduction and reduce furnace efficiency.

Both gas and solid temperature become uniform midway in the reduction zone. In the upper portion of the zone, the incoming oxide pellets tend to attain the much higher temperature of the reducing gas. This observation is in line with the observations of [15].

V. CONCLUSION

Mathematical models describing the multiple gas solid reactions, the physico-chemical, transport and thermal phenomena taking place in the Direct reduction furnace of the Delta Steel plant have been developed. The shrinking core model was used while modeling the non-catalytic gas-solid reactions. The models were validated with data obtained in the reduction of the local Itakpe iron ore pellets. The effect of the diffusion resistances, the intra-particle diffusion and kinetic phenomena coupled with other operating parameters on the overall particle

conversion were examined and the SCM was able to correctly describe the heterogeneous process. The results of the reduction of the Itakpe iron ore were in close conformance with the behaviour of most worldwide iron oxides used in the direct reduction process

VI. REFERENCES

(1) Madagua A. A, The betrayal of the Nigerian steel dream-Delta steel company saga; Bosem Publishers, Nigeria. 2013

(2) Ola S.A., Usman G. A., Odunaike A. A., Kollere S. M., Ajiboye P. O., and Adeleke A. O., Pilot Scale Froth Flotation Studies To Upgrade Nigerian Itakpe Sinter Grade: *Journal of Minerals & Materials Characterization & Engineering*, Vol. 8, No.5, (pp 405-416). 2009

(3) Akpah, F. A, Hydrogeochemistry and Impact of Iron Ore Mining on groundwater Quality in Itakpe and its Environs, Kogi State, Central Nigeria, MSc. University of Nigeria, Nsukka. 2008

(4) Ameh, E. G, Geochemical Distribution of Heavy Metals in Soil around Itakpe Iron-ore Mining Area-a Statistical Approach, *Research Journal of Environmental and Earth Sciences*, 6(3), (pp118-126). 2014

(5) Akinrisola, E. O.and Adekeye, J.I.D., Statistical ore reserve estimation of the Itakpe iron ore deposit, Okene, Kogi state, *Journal of mining and Geology*, 29(1), (pp19-25), 1993

(6) Atsushi, H. U., and Takashi, S., Midrex Processes, Kobelco Technology Review No. 29. 2010

(7) Direct Reduction Plant Operating Manual, Vol. 1

1981

(8) Parisi, D. R., and Laborde, M. A., Modeling of Counter Current moving Bed Gas-Solid Reactor used in Direct Reduction of Iron Ore, *Chemical Engineering Journal*, 104, (pp35–43). 2004

(9) Szekely, J., Evans, J.W., and Sohn, H.Y., *Gas-solid Reactions*, Academic Press. (pp 8-131), 1976

(10) Perry, R. H., and Green, D. W. (eds), *Perry's Chemical Engineer's Handbook*, McGraw Hill, USA. 2008.

(11) Rahimi, A., and Niksiar, A., A general model for moving-bed reactors with multiple chemical reactions part I:Model formulation, *International Journal of Mineral Processing*, 124, (pp 58–66), 2013

(12) Himmelblau, D.M., and Riggs, J.B., *Basic Principles and Calculations in Chemical Engineering*, New Jersey, 1989

(13) Alamsari, B., Torii, S., Trianto, A., and Bindar, Y, Heat and Mass Transfer in Reduction Zone of Sponge Iron Reactor, *International Scholarly Research Network*, Vol. 2011, Article ID 324659. 2011

(14) Beheshti, R., Moosberg-Bustnes, J., and Aune, R. E., *Modeling and simulation of isothermal reduction of a single hematite pellet in gas mixtures of H2 and CO.* Paper presented at the TMS 2014: 143rd Annual Meeting & Exhibition. 2014

(15) Negri E.D., Alfano O.M., and Chiovetta M.G., Direct reduction of hematite in a moving bed. Comparison between on- and three interface pellet models, *Chemical Engineering Science*, 42, 2472-2475. 1987